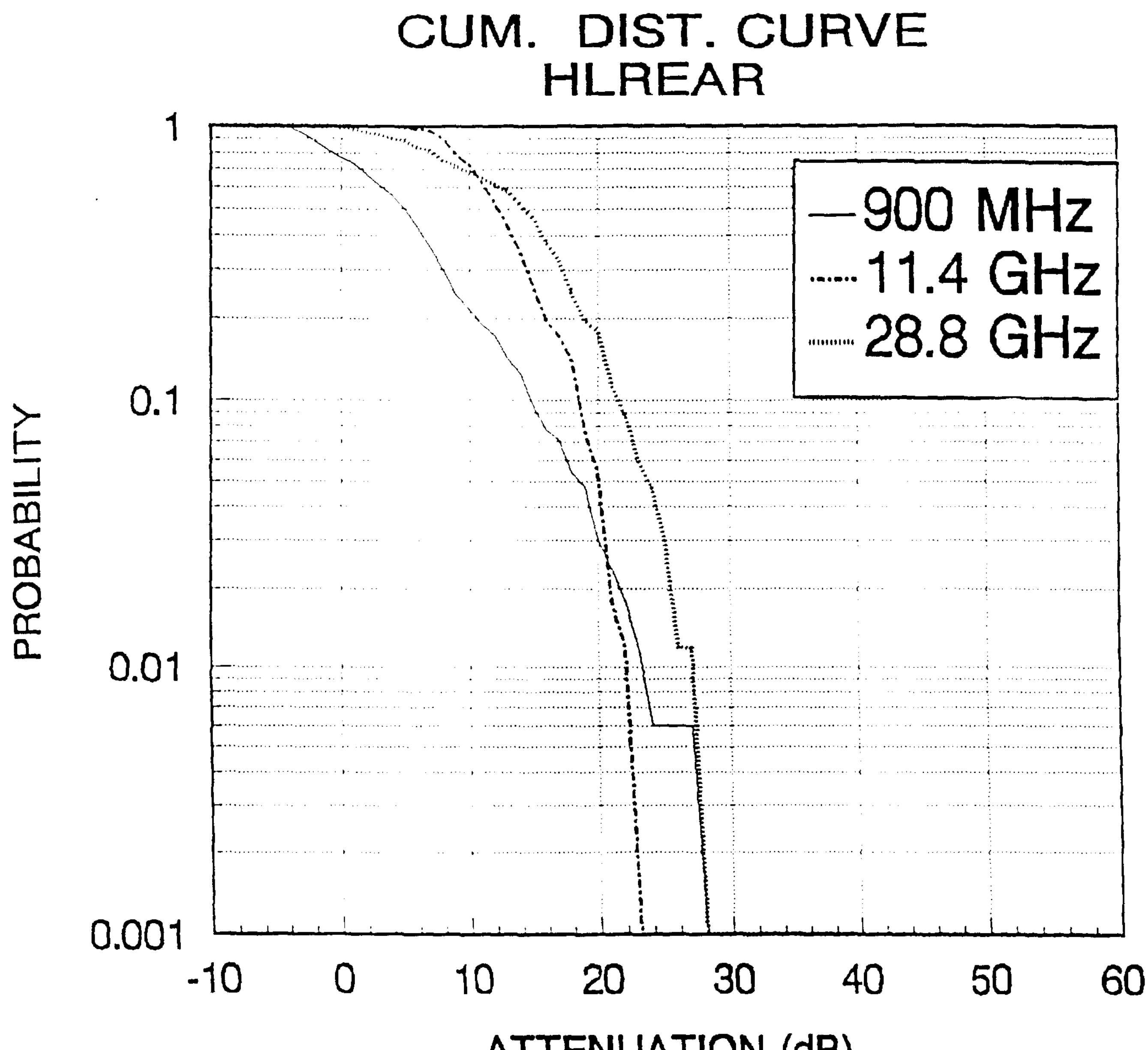

Figure 22. Cumulative distribution for all data in the private residence with two walls between the transmitter and receiver.

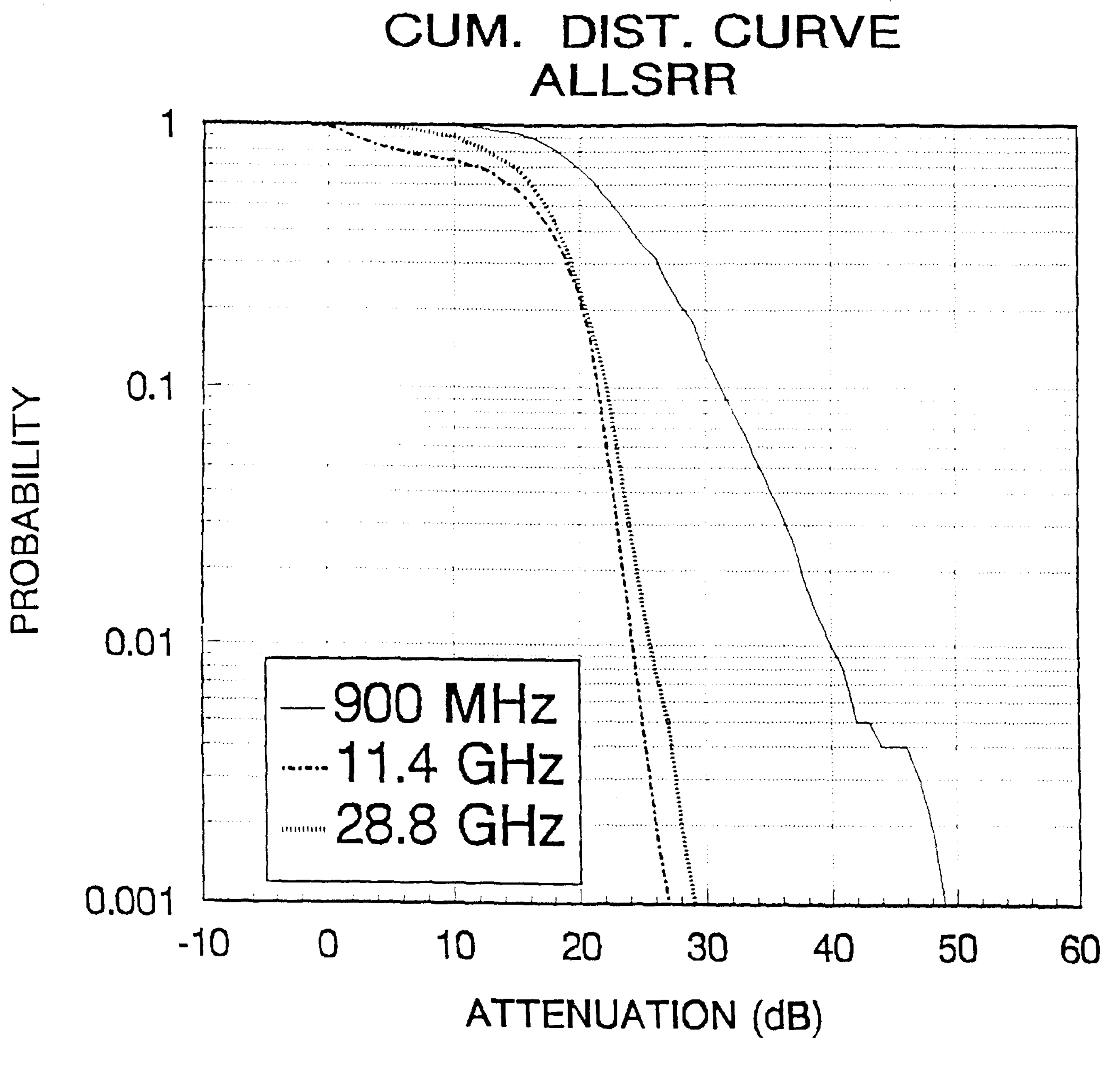

Figure 23. Cumulative distribution for all data in the storeroom building with metal siding.

The maximum attenuation that will be present less than a certain percentage of time can be read off these figures. This number can be used for the link margin at different link reliabilities. Table 4 has the mean attenuation and its standard deviation for all three data combinations. The means at all frequencies are greater for the two-wall case.

Figure 23 shows the cumulative distribution function for all of the data collected in the storeroom (metal structure with metal siding). The mean attenuation and its standard deviation are listed in Table 4. The attenuation is highest (greater than 49 dB less than 0.1 % of the time) at 900 MHz, because of the shielding effect of the metal siding on the building and the small windows (with respect to a wavelength at 900 MHz). The attenuation at 11.4 and 28.8 GHz was greater than 27 and 29 dB respectively less than 0.1 % of the time.

6.0 CONCLUSIONS

The penetration attenuation for the Radio Building and the private residence tend to increase with frequency. The penetration attenuation for the storeroom decreases with increasing frequency.

The separate cases for the Radio Building and private residence also indicate a progressively increasing amount of penetration attenuation at all frequencies as the number of wall penetrations increase in the building structure.

The electromagnetic energy at 11.4 and 28.8 GHz can couple into the storeroom building more effectively than that energy at 900 MHz. The shielding effectiveness (ratio in dB of the power outside the structure to the power inside the structure) of the structure is less at the two higher frequencies and allows more energy to couple through the walls. The shielding effectiveness of a metal structure is dependent on the size of the openings in the outer shell of the structure. These may be windows, doors, heating and/or air conditioning penetrations, holes, etc. When the size of the opening in the structure is greater than or comparable to a wavelength, then the opening in the structure provides a strong coupling path for electromagnetic energy to flow into or out of the structure. This reduces the penetration attenuation of the structure.

The penetration attenuation values derived from the measurements conducted in this study can be used determine the feasibility of personal communications. The cumulative distribution functions of the penetration attenuation can provide information on what link margins are necessary for different communication probabilities or reliabilities. The penetration attenuation provides a quantitative margin for link calculations to use in analyzing and designing personal communication systems.

APPENDIX: ATTENUATION PLOTS FOR ALL MEASUREMENT PATHS

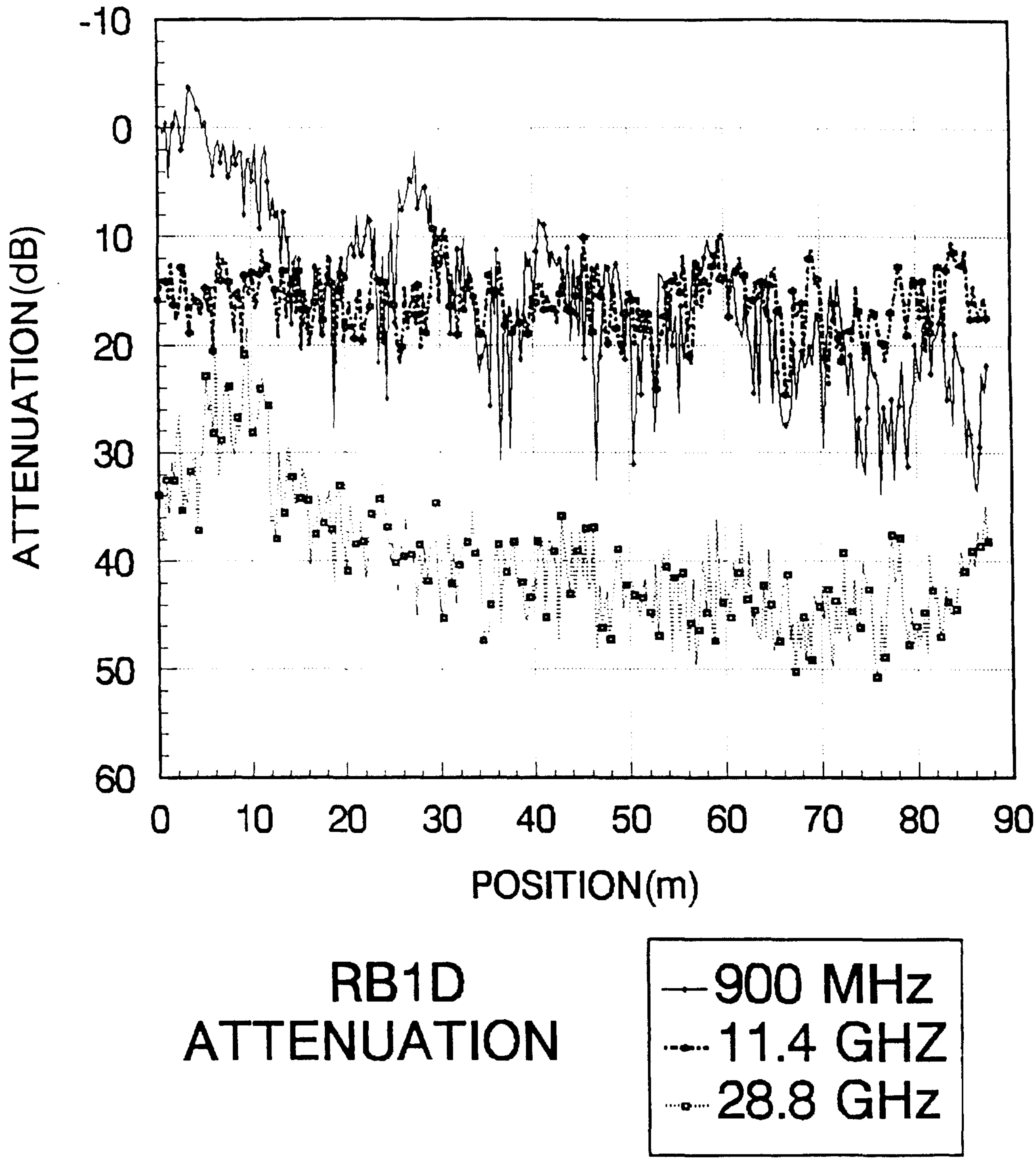

Figure A-1. Penetration loss for Radio Building path RB1D.

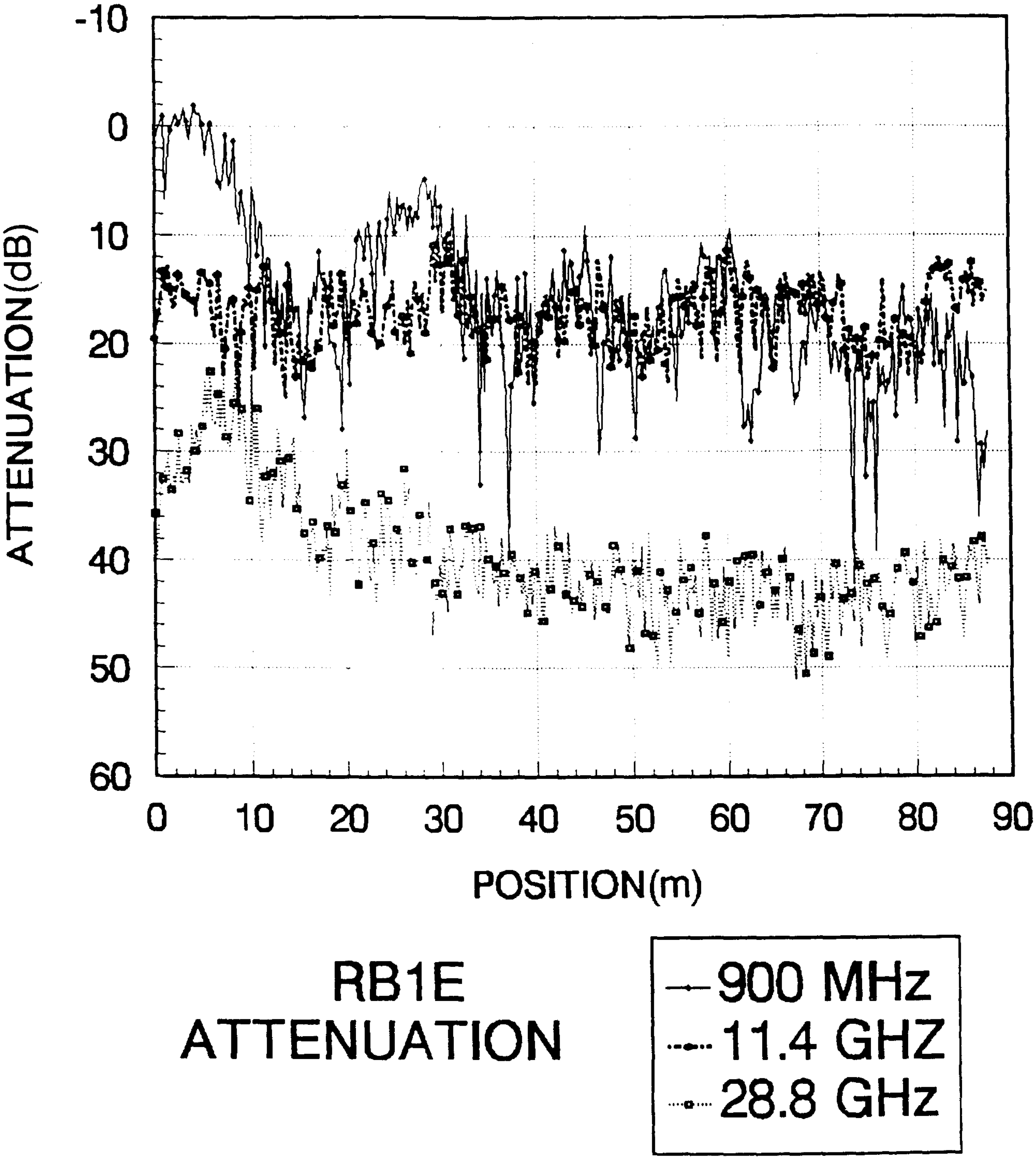

Figure A-2. Penetration loss for Radio Building path RB1E.

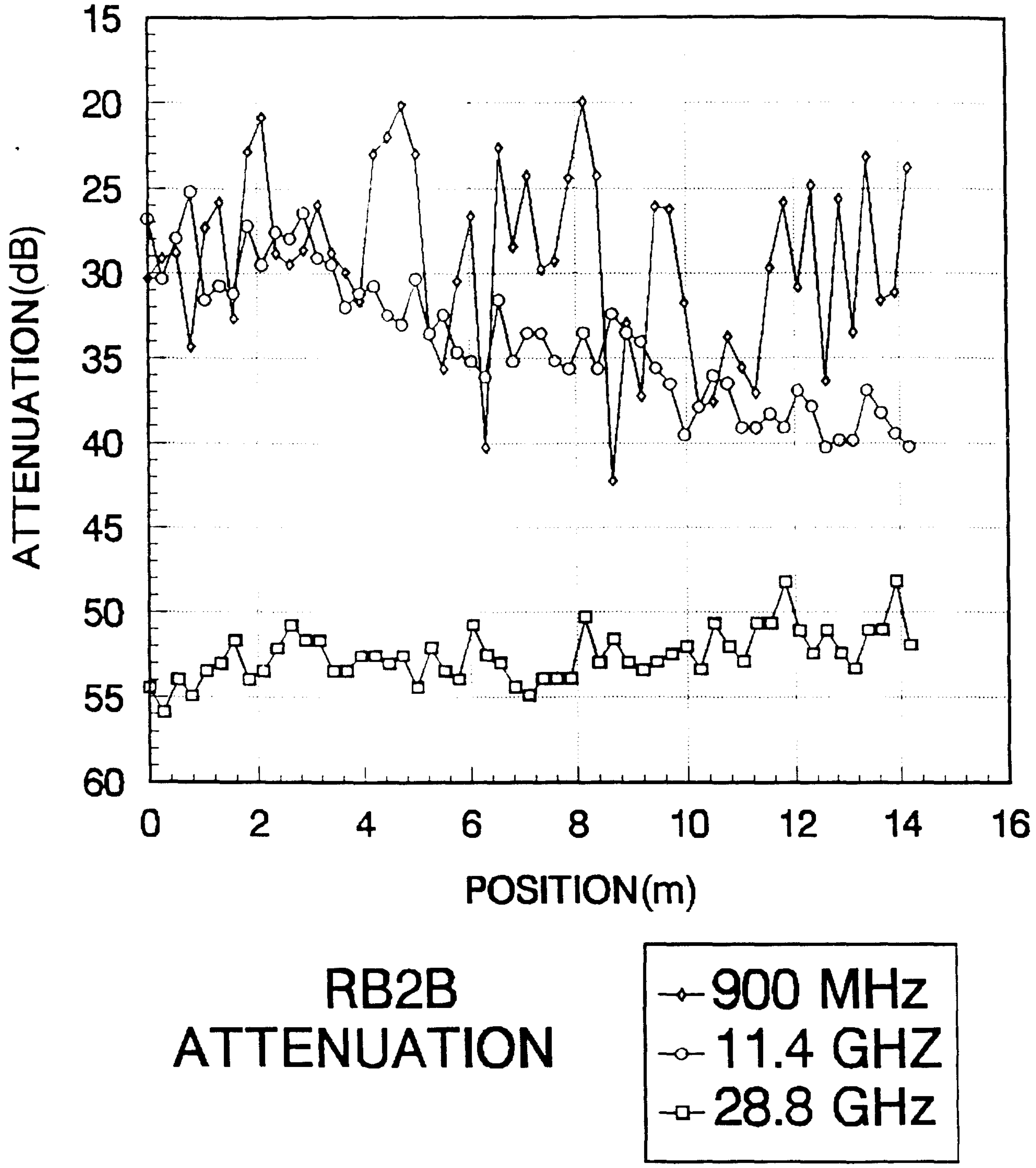

Figure A-3. Penetration loss for Radio Building path RB2B.

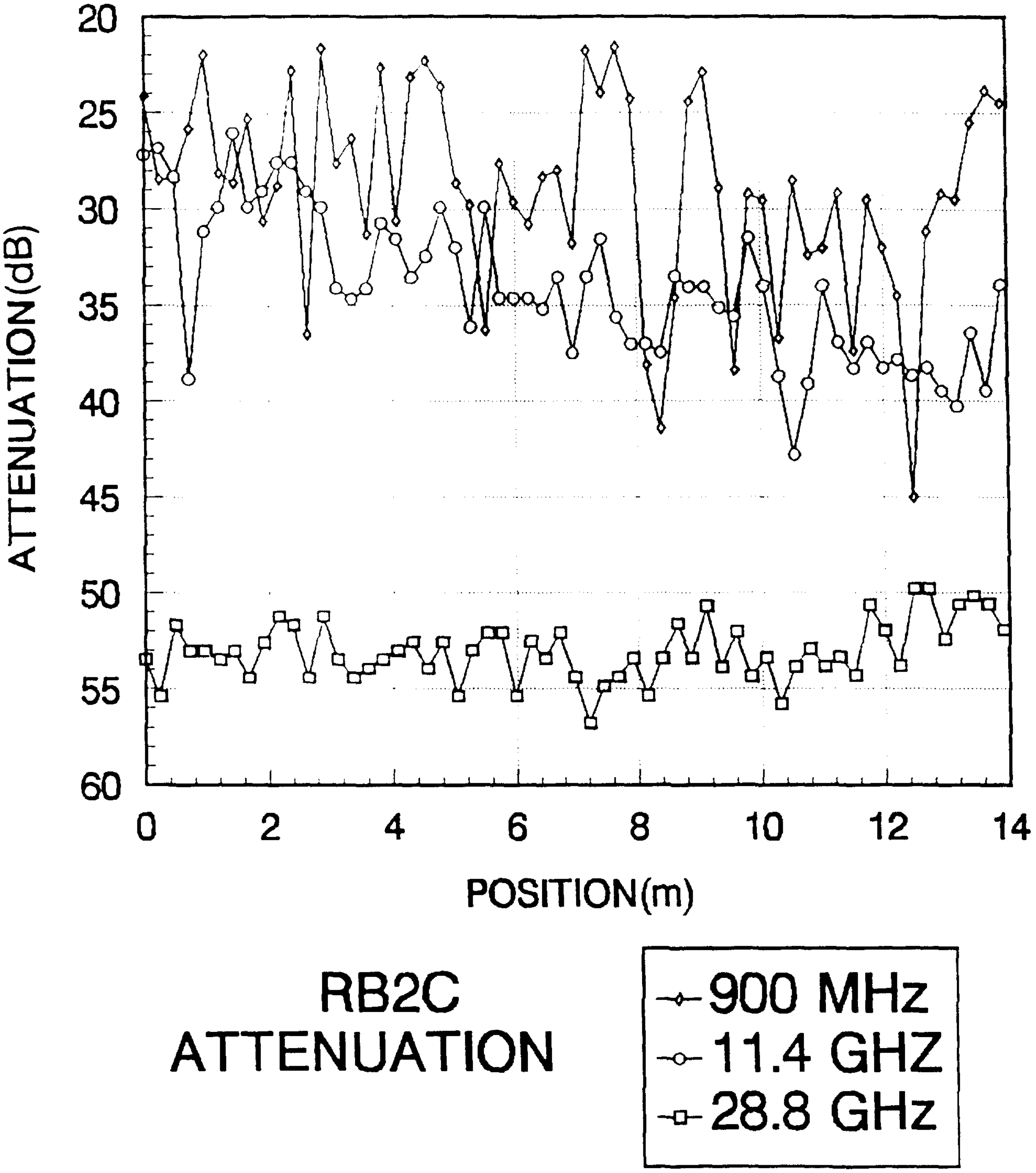

Figure A-4. Penetration loss for Radio Building path RB2C.

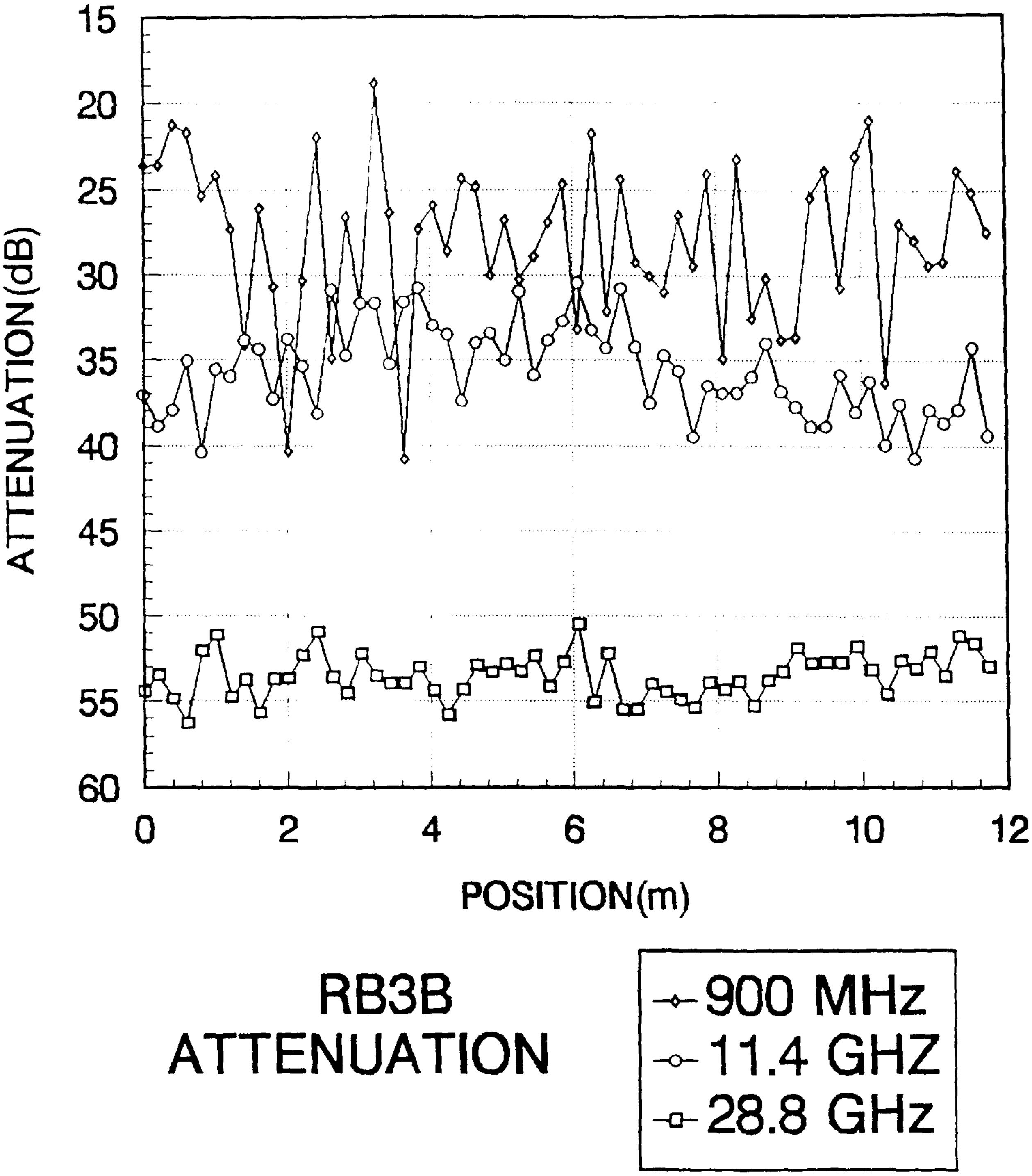

Figure A-5. Penetration loss for Radio Building path RB3B.

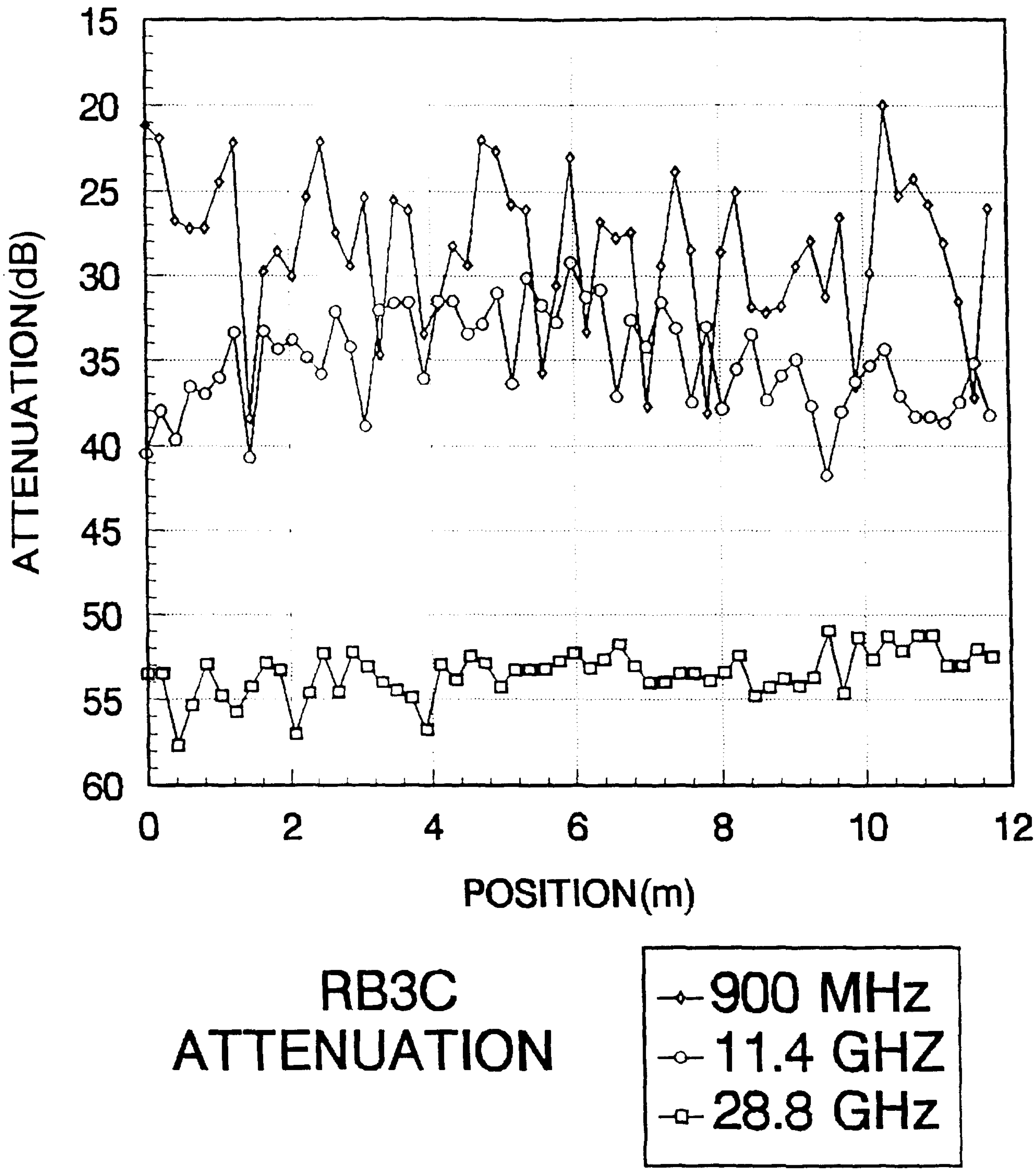

Figure A-6. Penetration loss for Radio Building path RB3C.

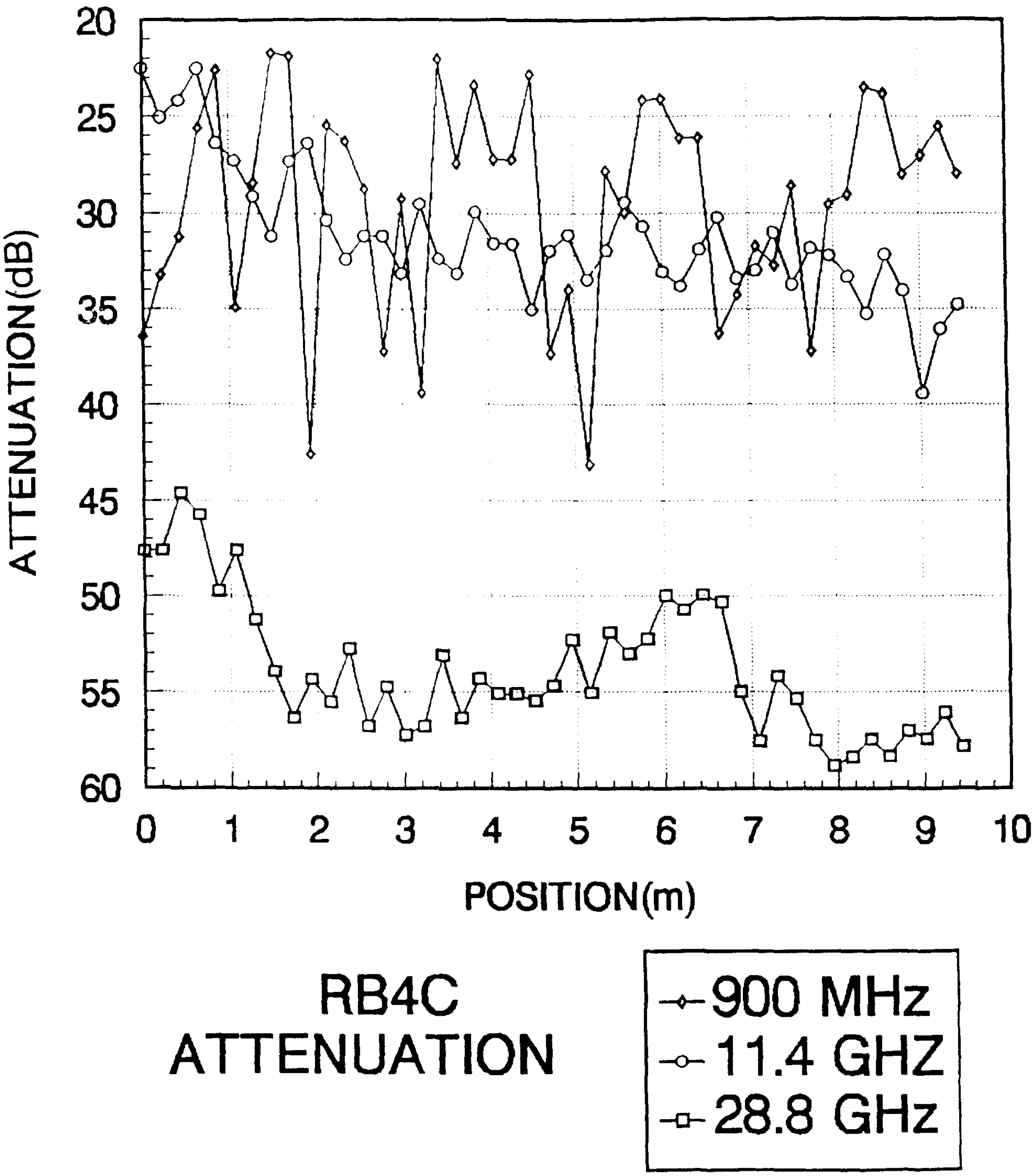

Figure A-7. Penetration loss for Radio Building path RB4C.

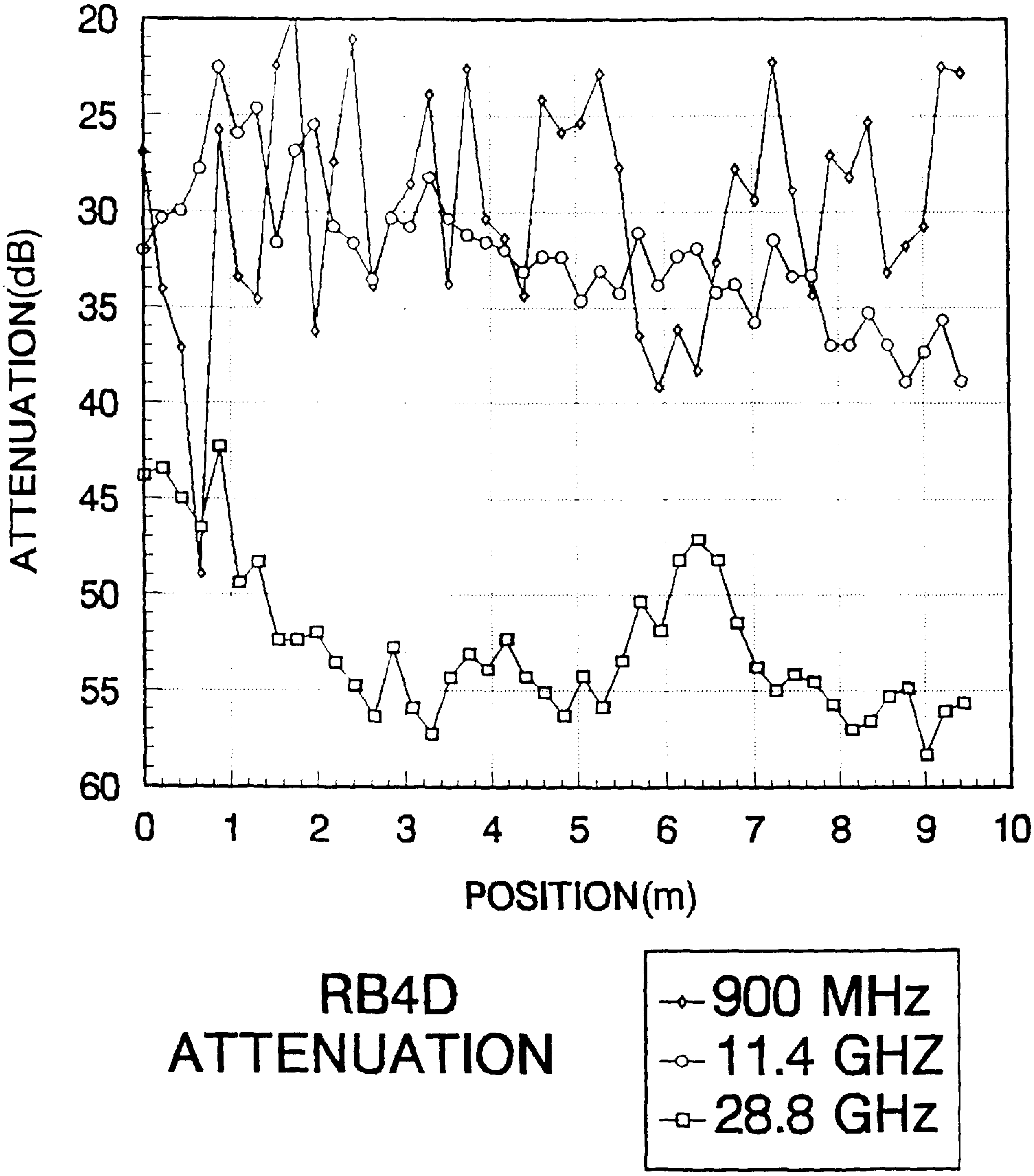

Figure A-8. Penetration loss for Radio Building path RB4D.

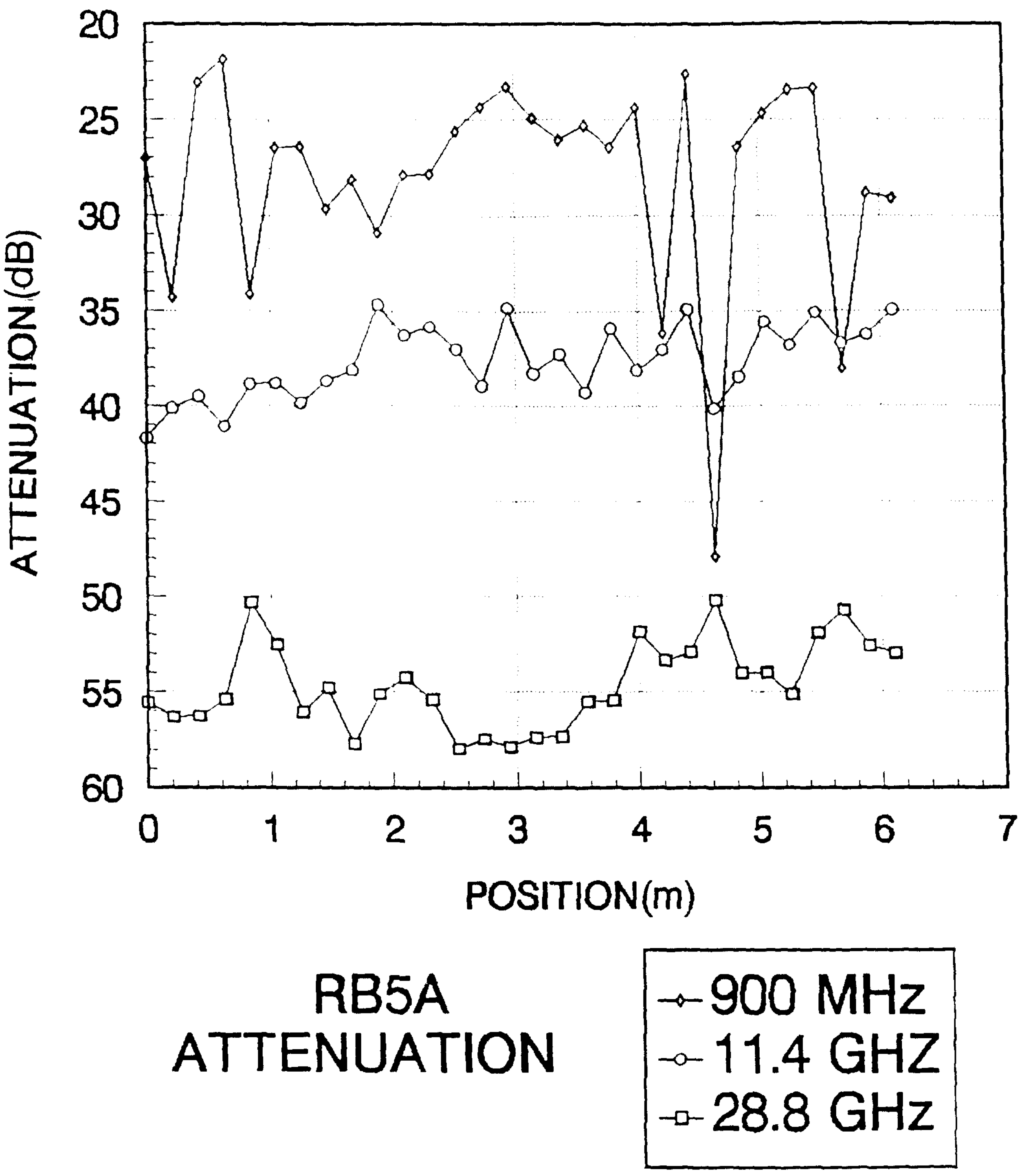

Figure A-9. Penetration loss for Radio Building path RB5A.

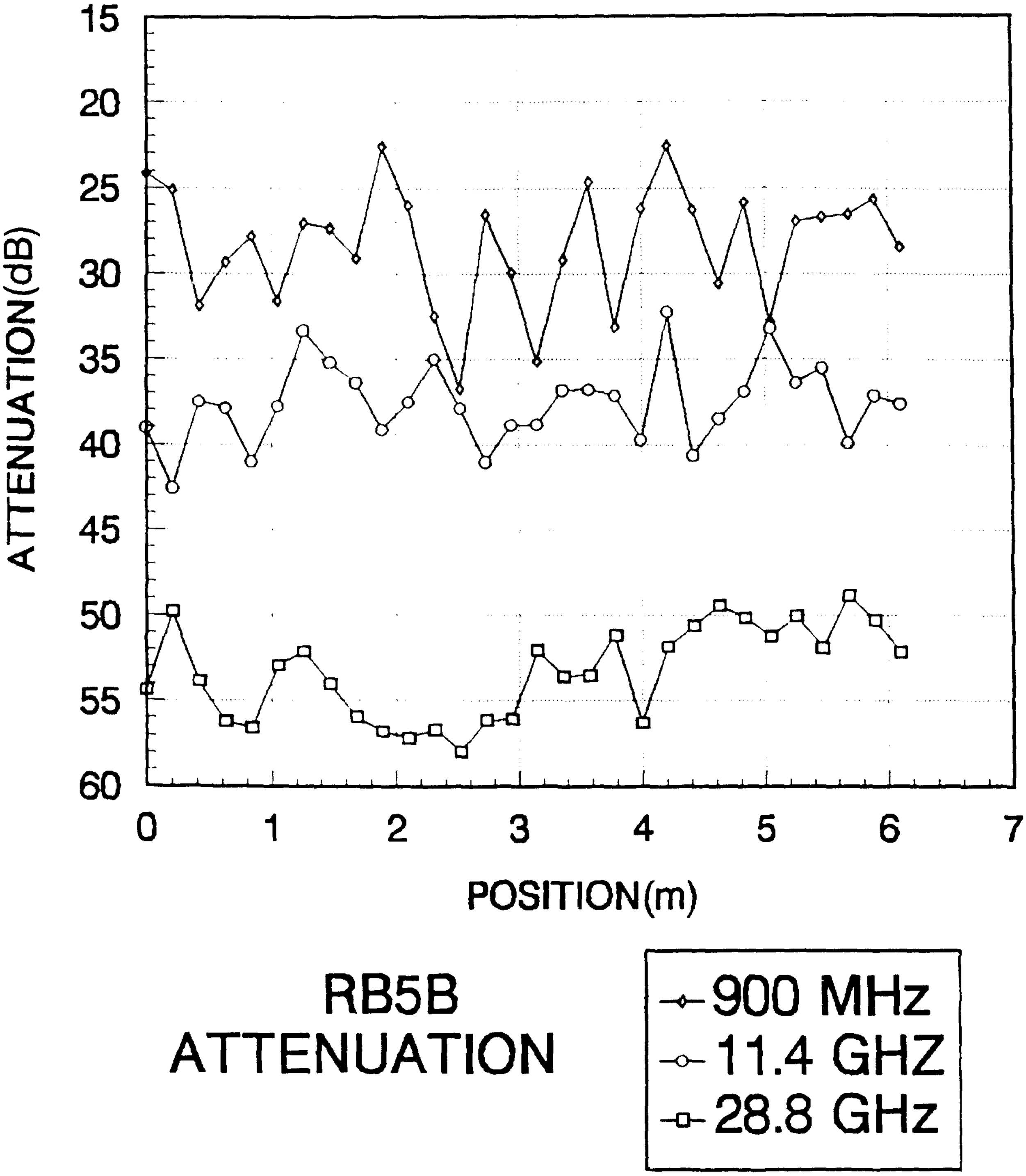

Figure A-10. Penetration loss for Radio Building path RB5B.

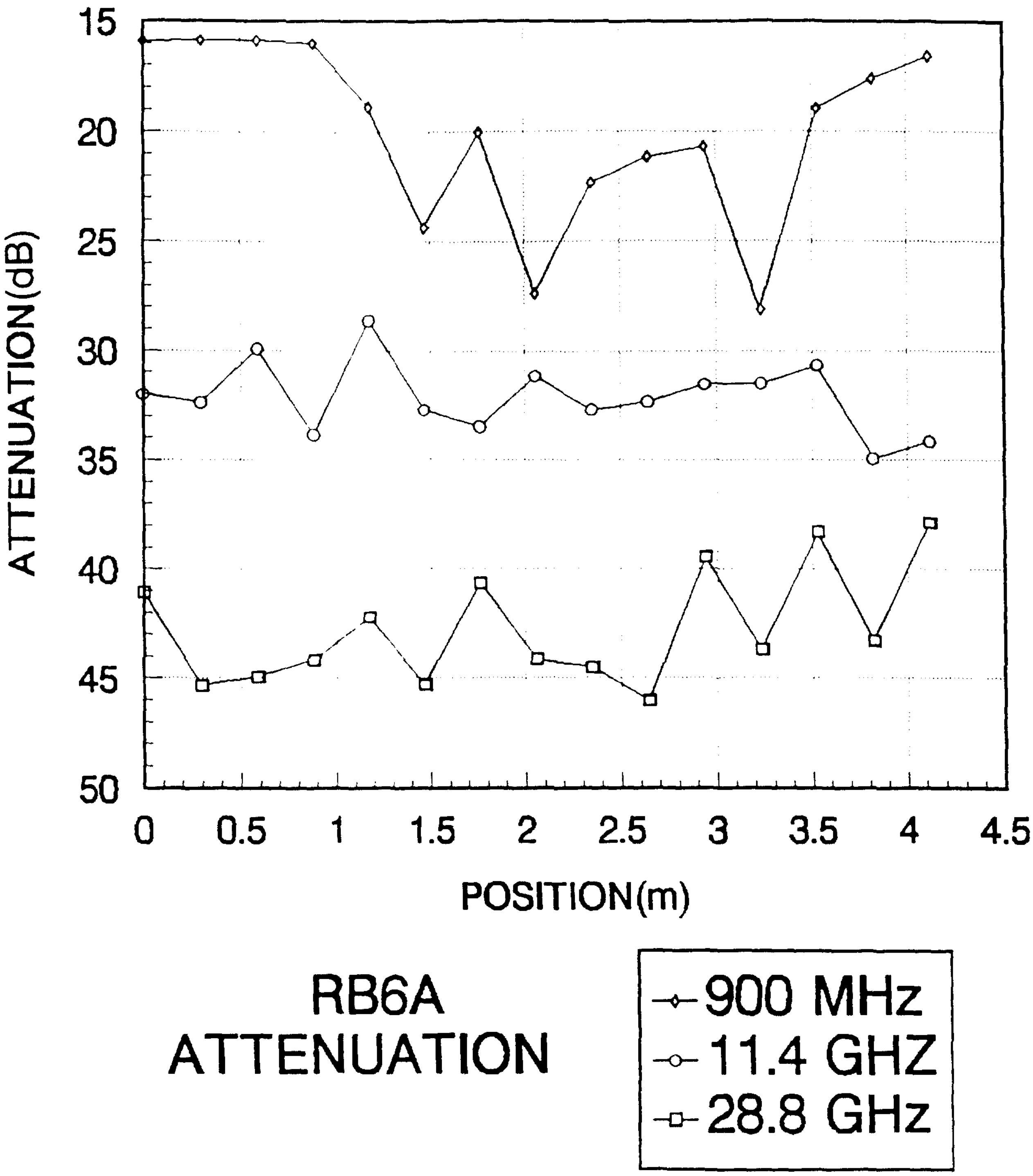

Figure A-11. Penetration loss for Radio Building path RB6A.

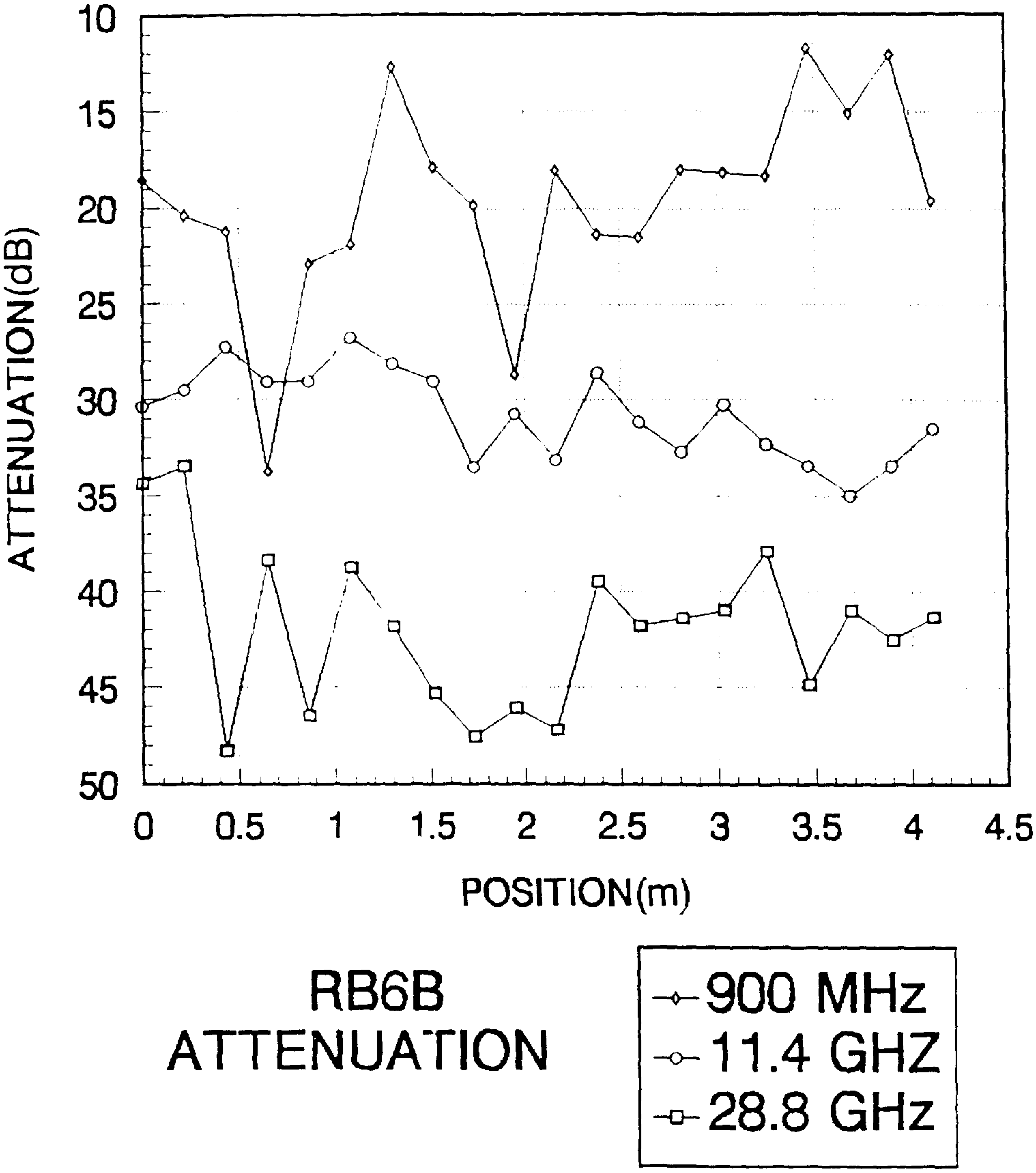

Figure A-12. Penetration loss for Radio Building path RB6B.

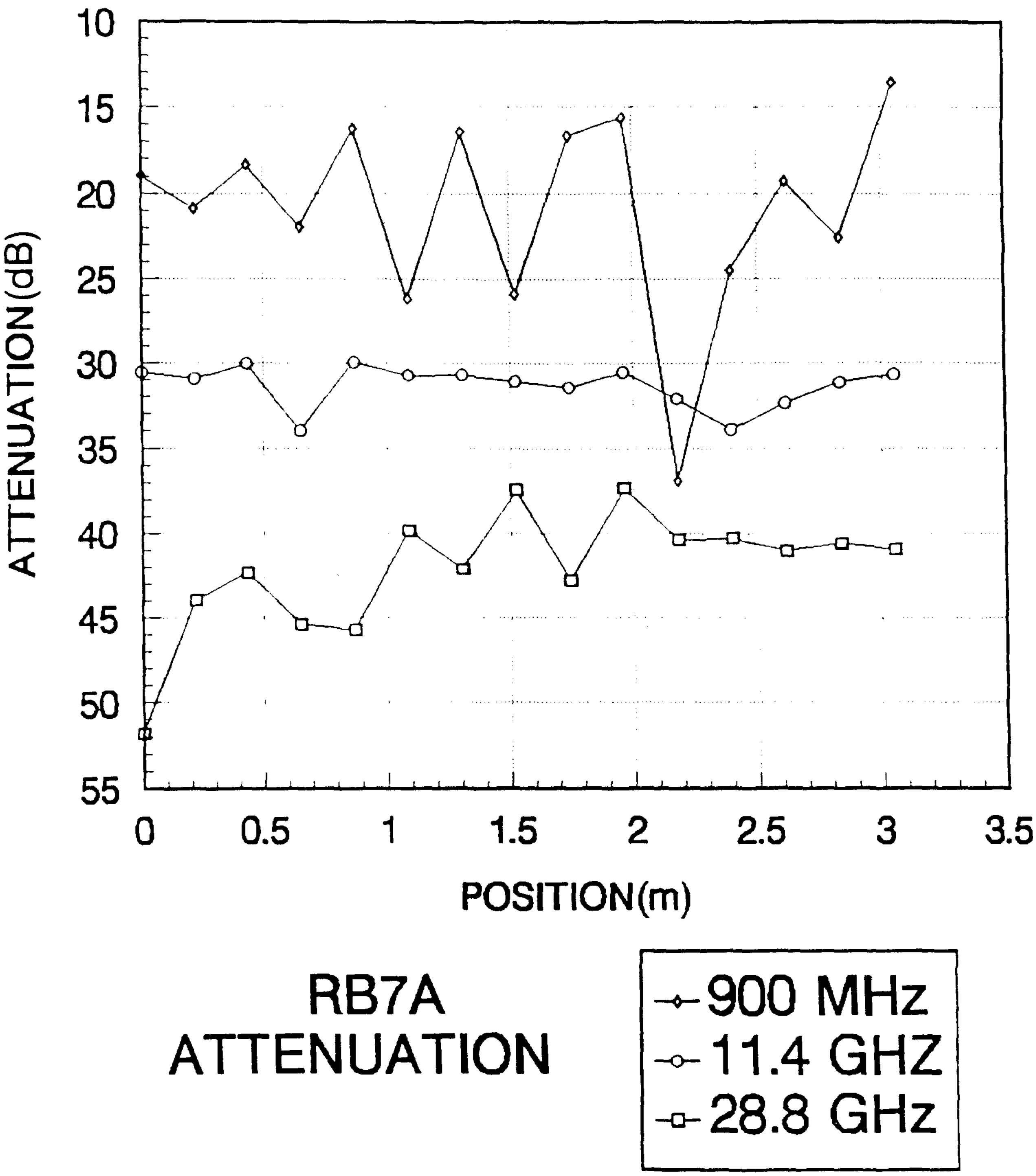

Figure A-13. Penetration loss for Radio Building path RB7A.

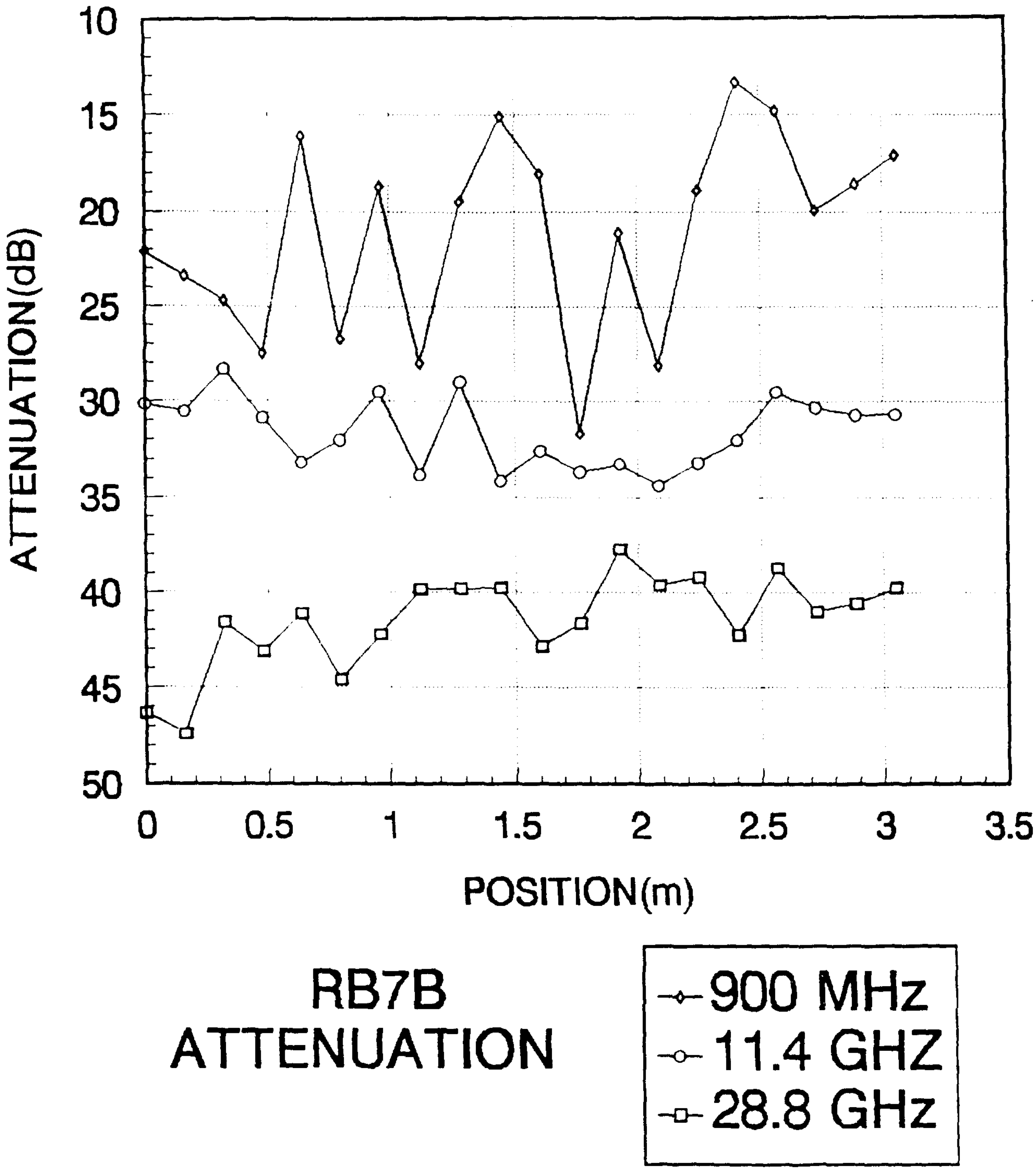

Figure A-14. Penetration loss for Radio Building path RB7B.

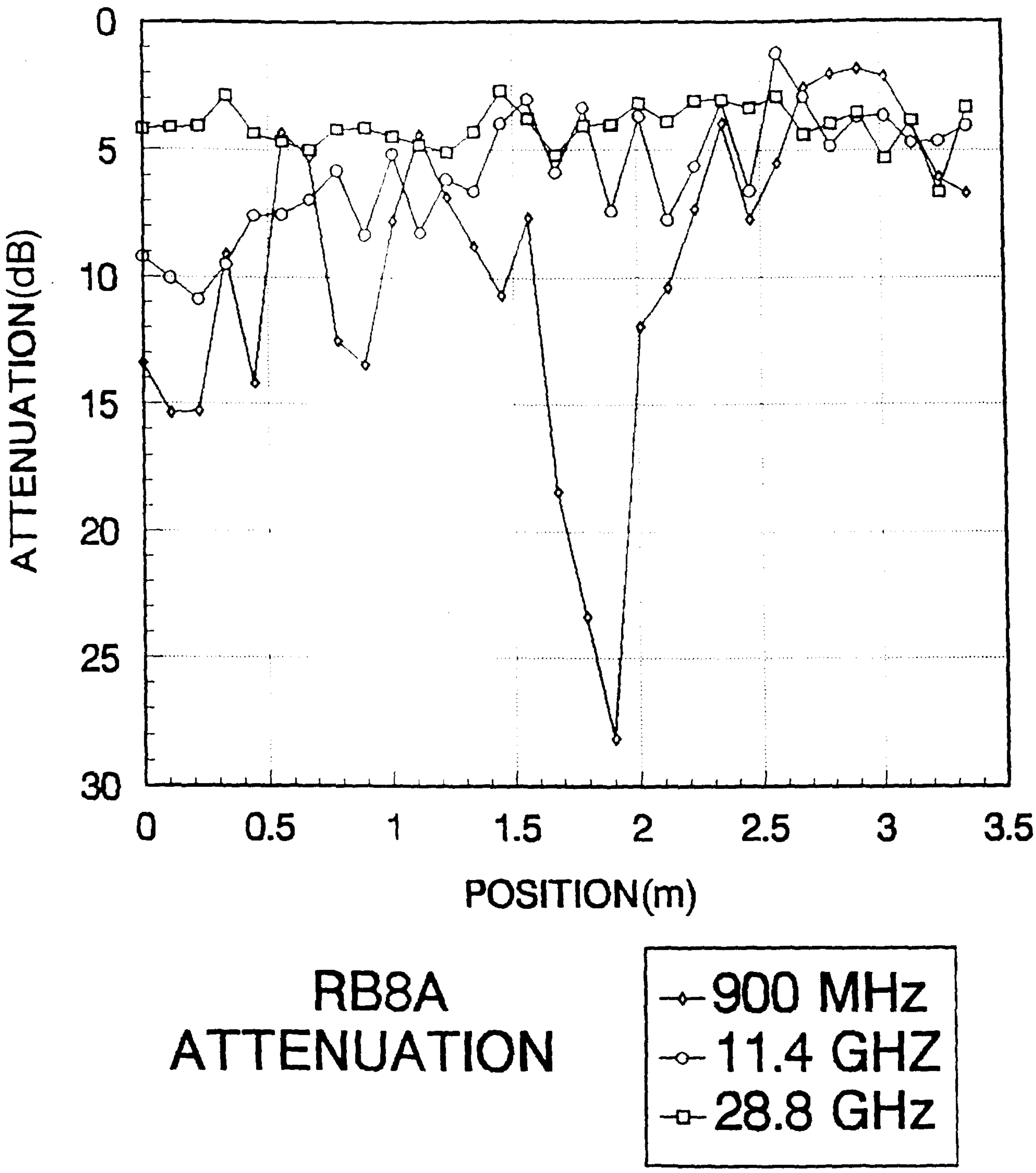

Figure A-15. Penetration loss for Radio Building path RB8A.

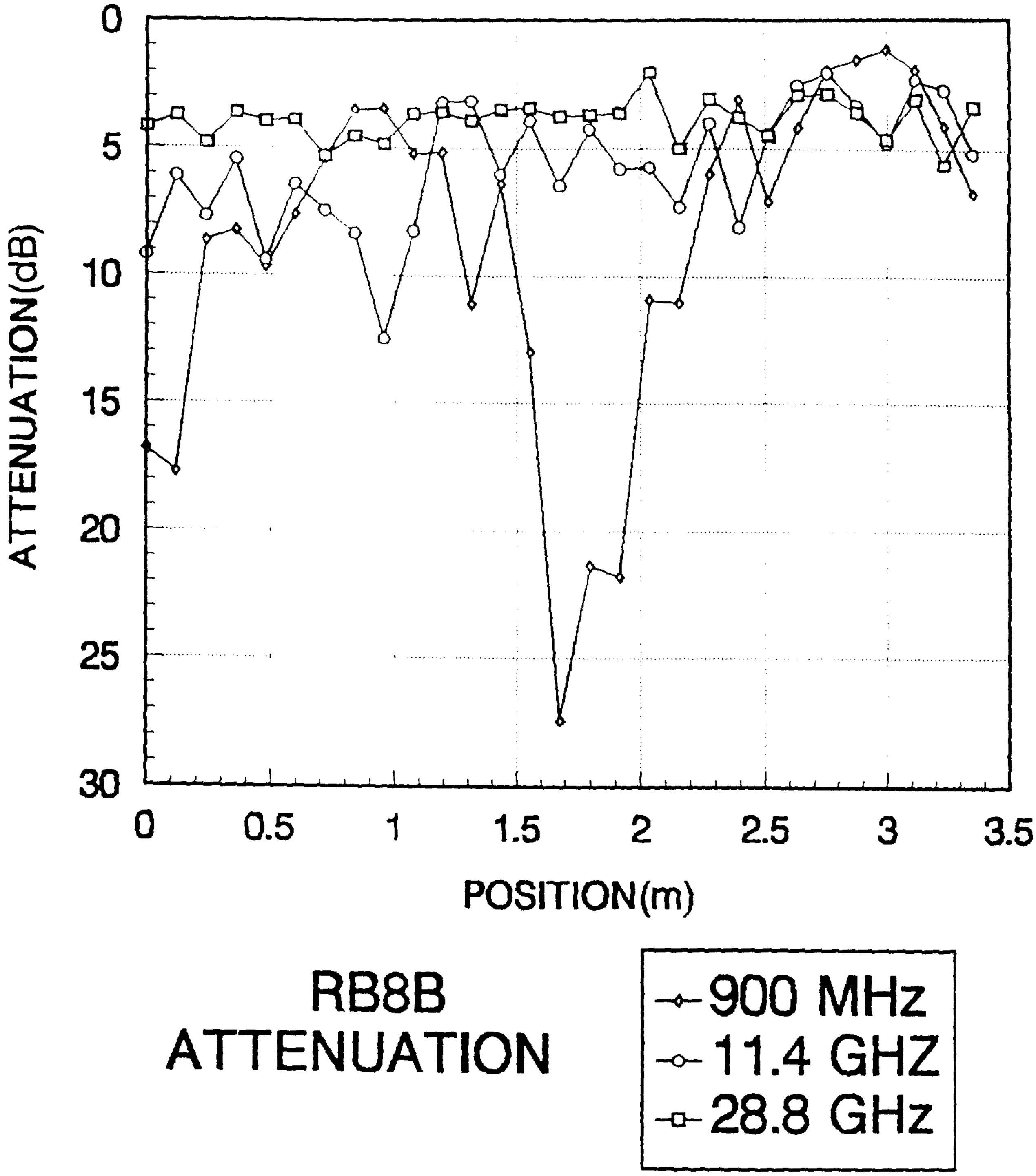

Figure A-16 Penetration loss for Radio Building path RB8B.

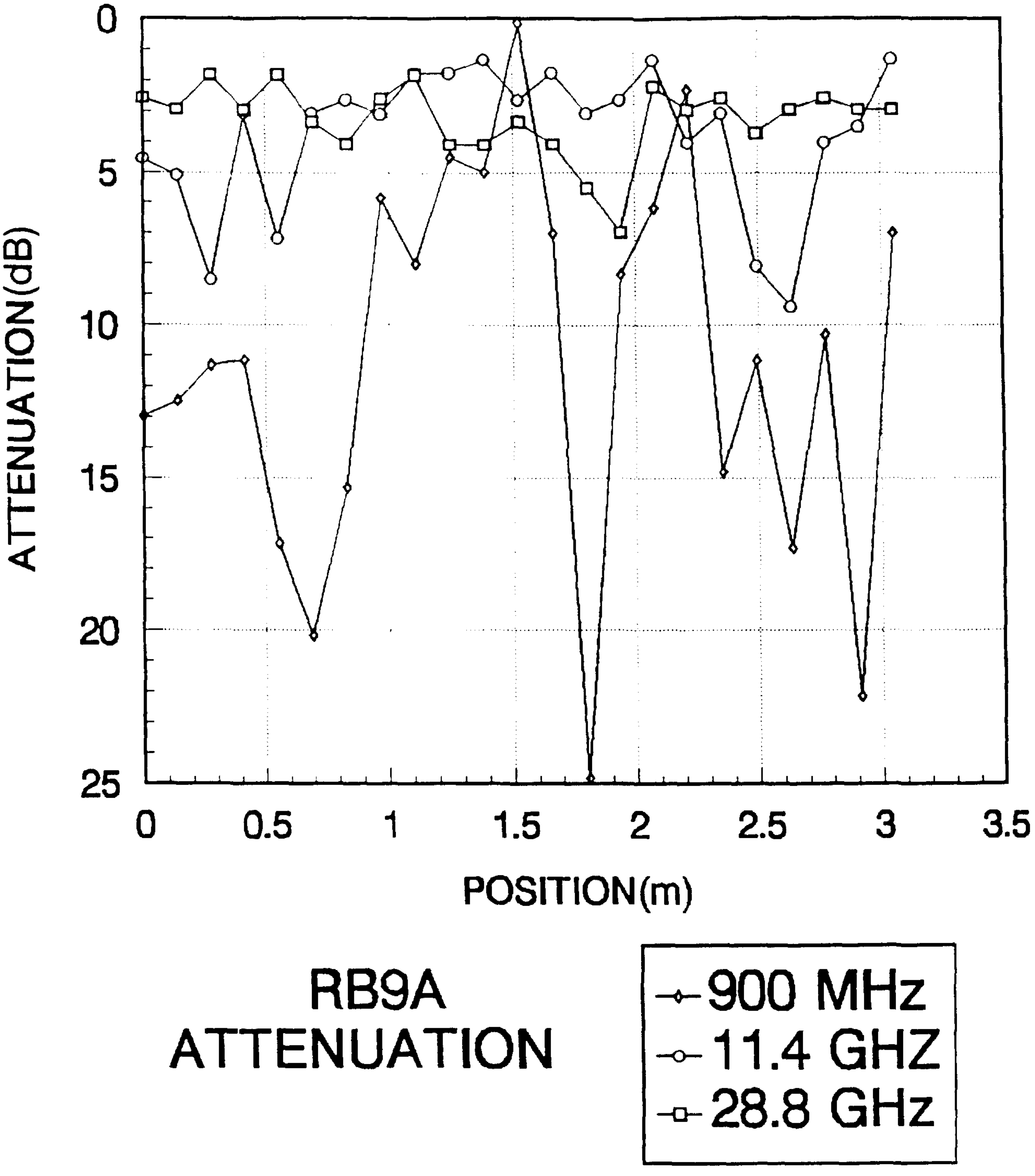

Figure A-17. Penetration loss for Radio Building path RB9A.

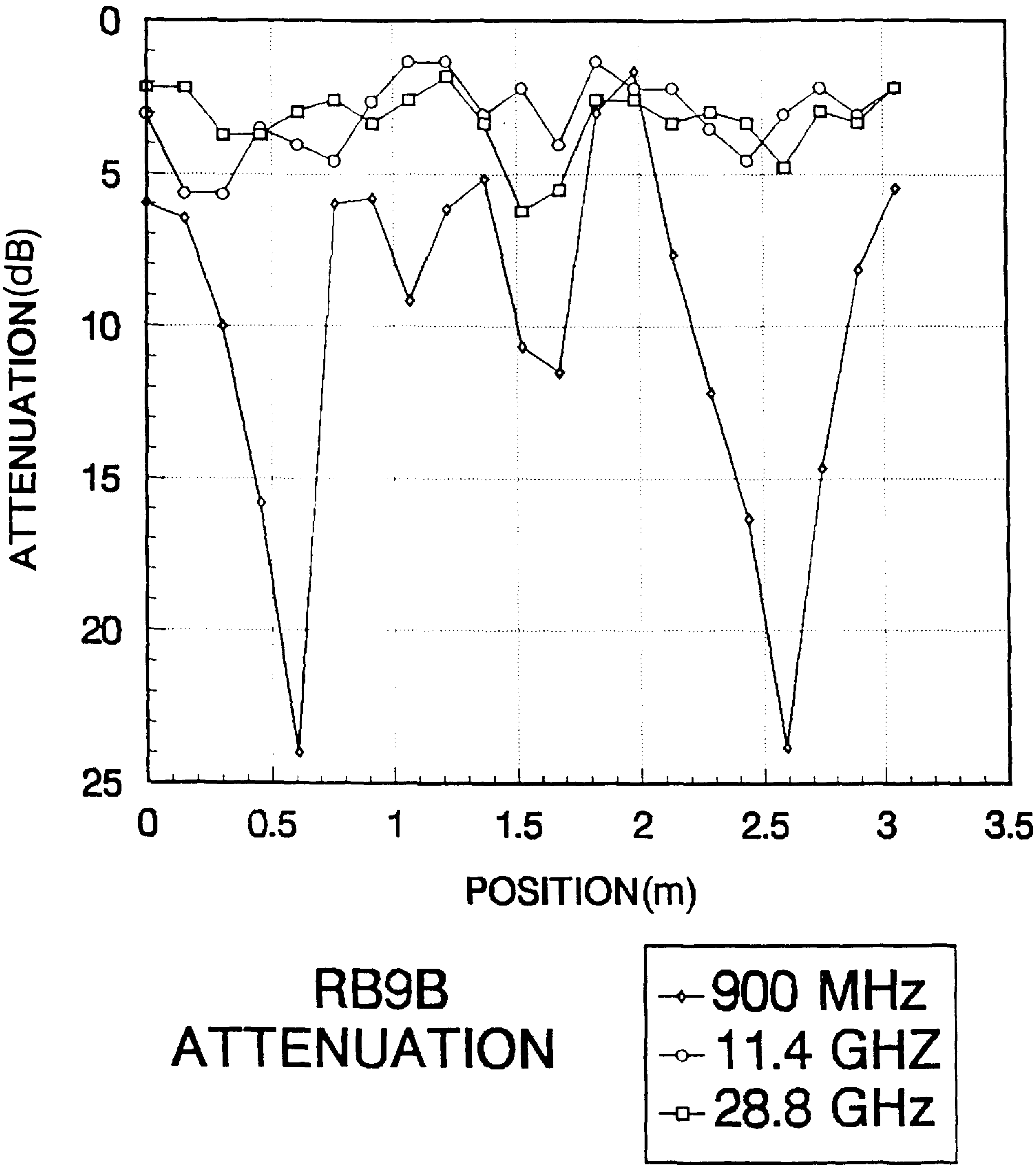

Figure A-18. Penetration loss for Radio Building path RB9B.

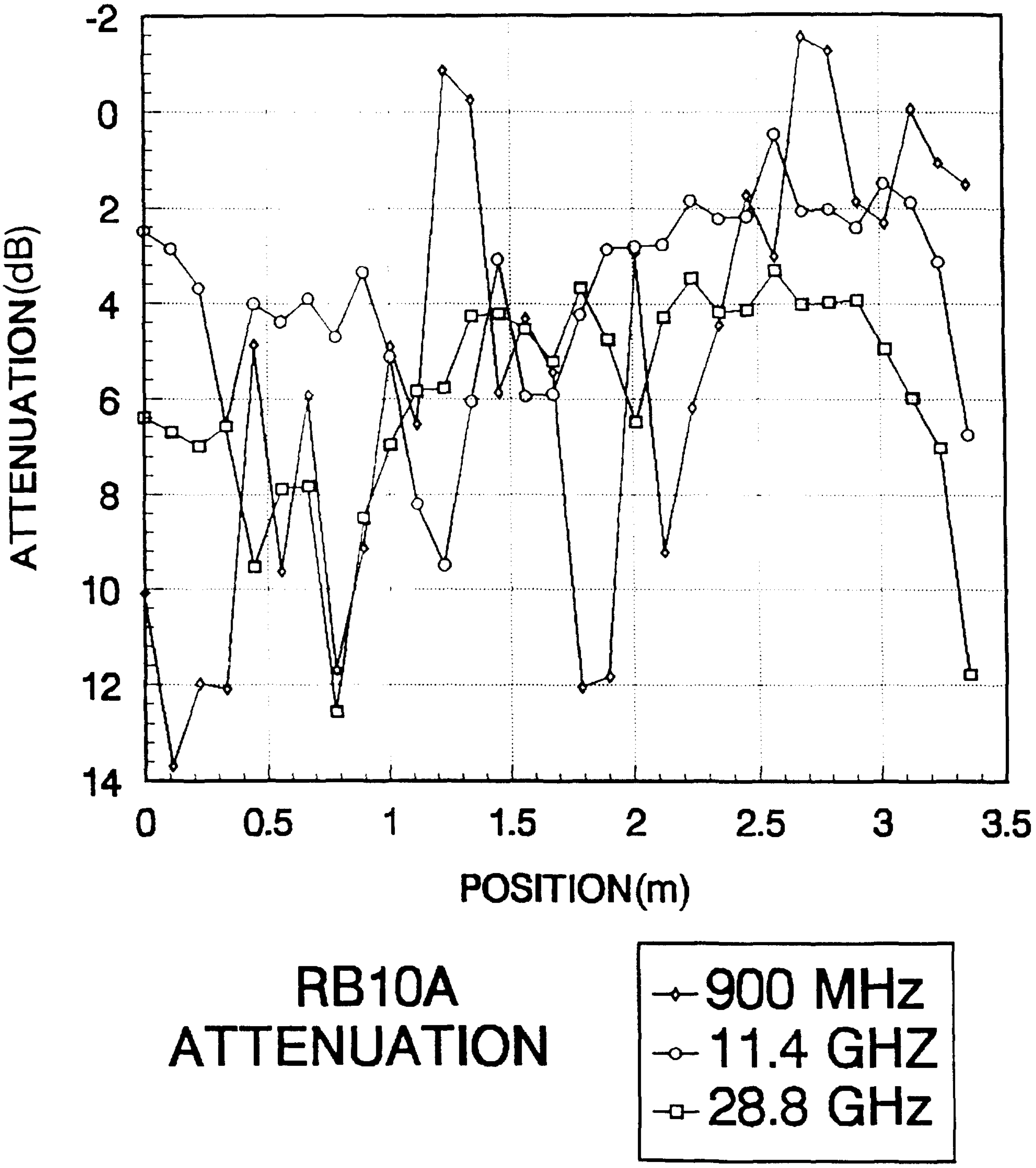

Figure A-19. Penetration loss for Radio Building path RB10A.

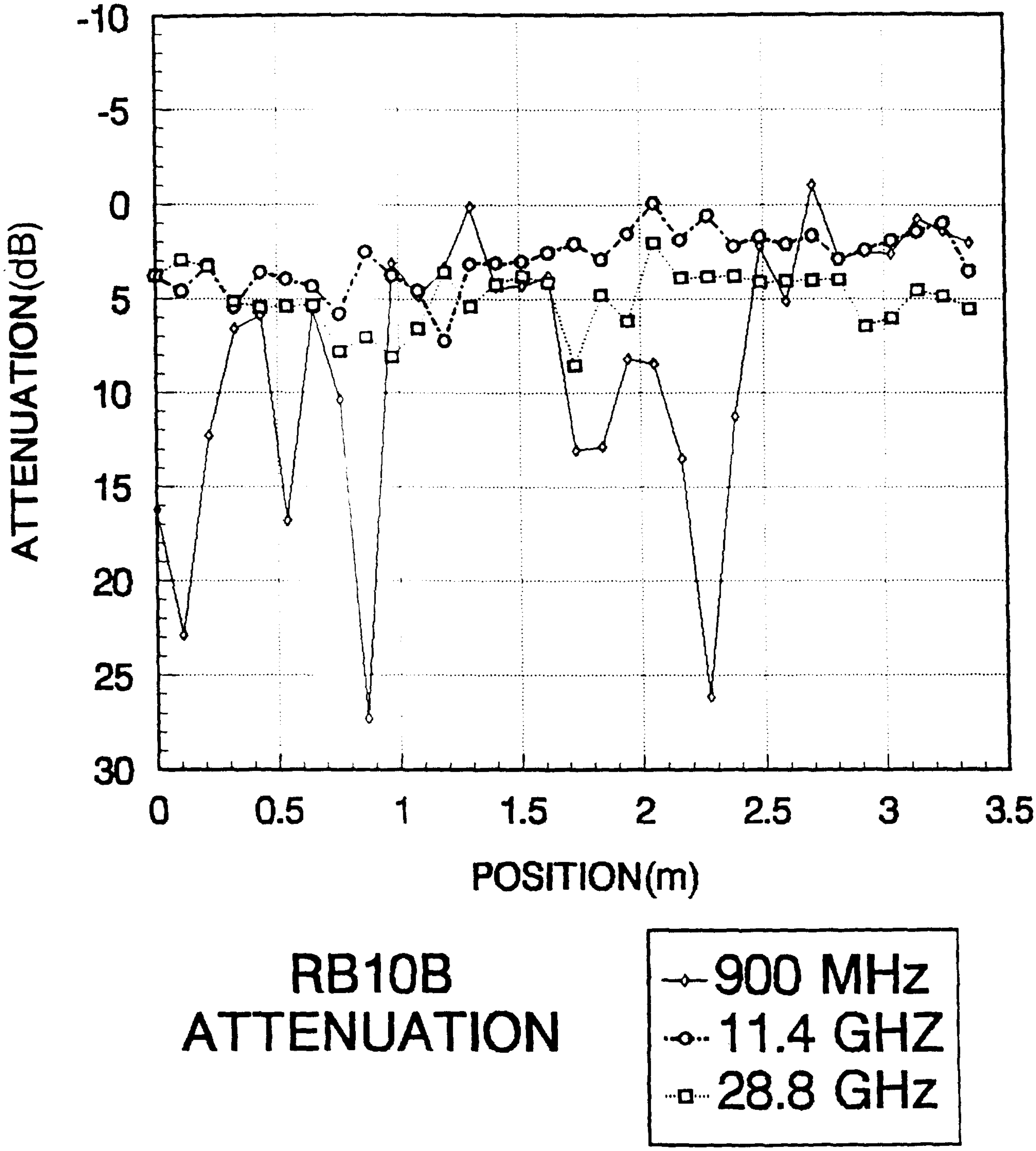

Figure A-20. Penetration loss for Radio Building path RB10B.

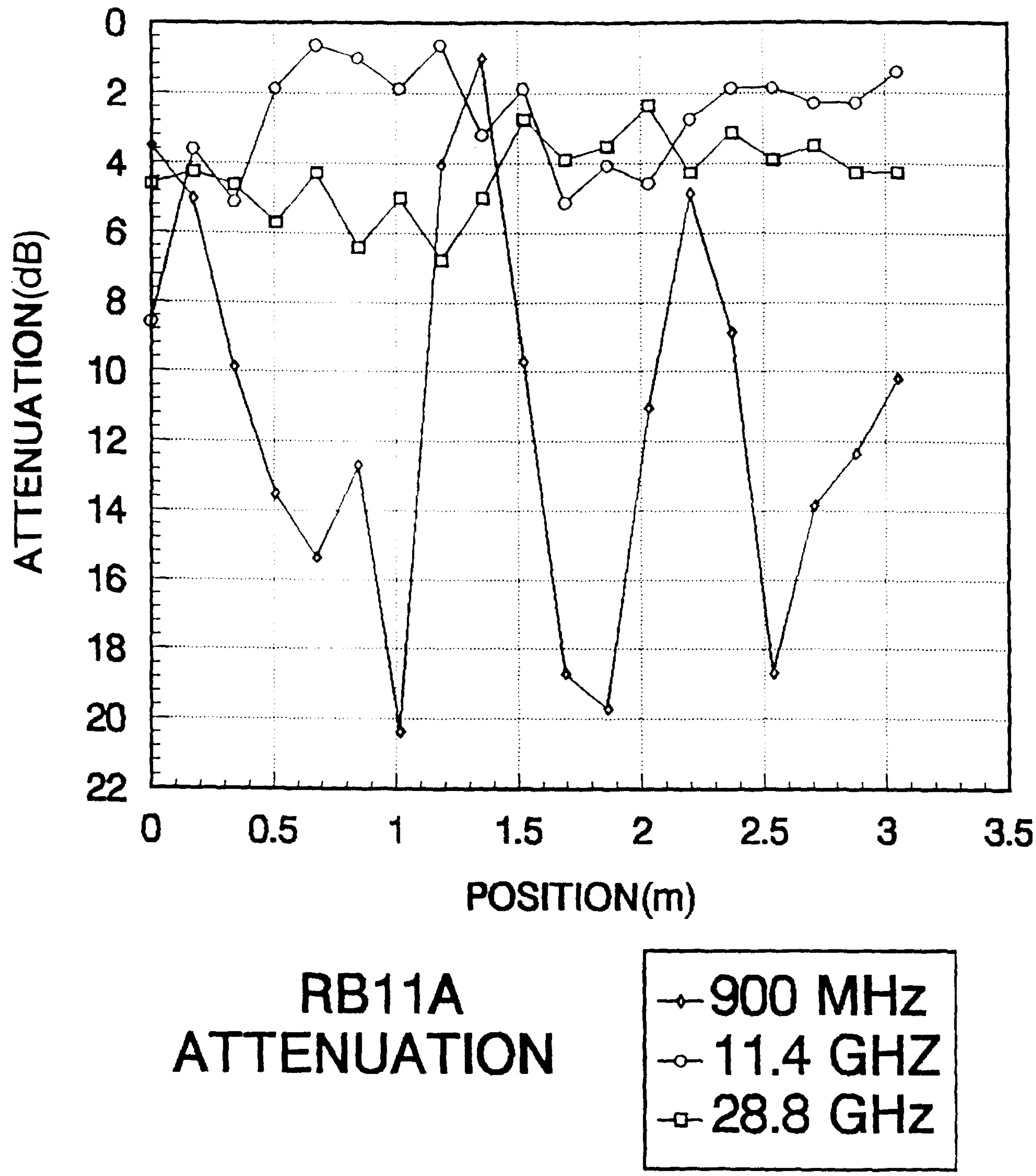

Figure A-21. Penetration loss for Radio Building path RB11A.